# Quantitative magnetization transfer of white matter tracts correlates with diffusion tensor imaging indices in predicting the conversion from mild cognitive impairment to Alzheimer's disease

Article (Accepted Version)

# Quantitative magnetization transfer of white matter tracts correlates with DTI indices in predicting the conversion from mild cognitive impairment to Alzheimer's disease

Elena Makovac[1], Laura Serra[1], Carlotta Di Domenico[1], Camillo Marra[2], Carlo Caltagirone[3,4], Mara Cercignani[1,5], Marco Bozzali[1,5]

[1] Neuroimaging Laboratory, IRCCS Santa Lucia Foundation, Rome;

[2] Institute of Neurology, Catholic University, Rome

[3] Department of Clinical and Behavioural Neurology, IRCCS Santa Lucia Foundation, Rome

[4] Department of Systems Medicine University of Rome 'Tor Vergata', Rome.

[5] Department of Neuroscience, Brighton & Sussex Medical School, University of Sussex, Brighton, United Kingdom.

**Running Title: qMT and DTI biomarkers of MCI conversion**

**Dr. Marco Bozzali**, Department of Neuroscience, Brighton and Sussex Medical School, University of Sussex, Brighton, East Sussex, BN1 9RH, UK. Telephone number: +44(0) 1273 873509; Fax number: +44 (0) 1273 876721; E mail address: m.bozzali@bsms.ac.uk

| |
|---|
| Abstract word count: 193 |
| Text word count: 4445 |
| No. Figures: 3 |
| No. of Tables: 3 |
| Title characters count: 22 |

**Abstract**

Patients with amnestic mild cognitive impairment (aMCI) have higher probability to develop Alzheimer's disease (AD) than elderly controls. The detection of subtle changes in brain structure associated with disease progression and the development of tools to identify patients at high risk for dementia in a short time is crucial. Here, we used probabilistic WM tractography to explore microstructural alterations within the main association, limbic and commissural pathways in aMCI patients who converted to AD after 1 year follow-up ($MCI_{converters}$) and those who remained stable ($MCI_{stable}$). Both diffusion tensor imaging (DTI) and quantitative magnetization transfer (qMT) parameters have been considered for a comprehensive pathophysiological characterization of the WM damage. Overall, specific tract-specific parameters derived from qMT and DTI at baseline were able to differentiate aMCI patients who converted to AD from those who remained stable in time. In particular, the qMT exchange rate, $RM^{B}_{0}$, of the right uncinate fasciculus was significantly decreased in $MCI_{converters}$, whereas fractional anisotropy (FA) was significantly decreased in the bilateral superior cingulum in $MCI_{converters}$ compared to $MCI_{stable}$. These results confirm the involvement of WM and particularly of association fibers in the progression of AD, highlighting disconnection as a potential mechanism.

**Keywords**: Mild cognitive impairment, quantitative magnetization transfer, diffusion tensor imaging, white matter, probabilistic tractography

## Introduction

Mild cognitive impairment of amnesic type (aMCI) is considered a pre-dementia phase, highly predictive of subsequent conversion to Alzheimer's disease [1]. Nonetheless, aMCI is a fairly heterogeneous condition [2 - 3], including not only patients at an early AD stage, but also patients who will remain stable, and patients at risk for developing other forms of dementia [4]. Determining the biophysical sensitivity and specificity of quantitative magnetic resonance imaging to AD pathology is essential to develop effective imaging biomarkers of neurodegeneration. While regional assessments of grey matter (GM) atrophy are sensitive to macroscopic changes occurring at relatively advanced phases of the disease [5 - 6], this approach is unable to highlight microstructural alterations that accompany and may well precede volume loss. The hypothesis that disconnection may be a contributor to the spread of damage in AD brains is increasingly gaining consensus [7], thus implying that early changes within the white matter (WM) tracts might play a crucial role in the onset and early progression of AD [7 - 9], up to the hypothesis that myelin breakdown might be implicated in the pathogenesis of AD [10]. This view is supported by evidence of microstructural changes occurring in the WM already in pre-clinical stages of AD [11]. It still remain to be established, however, whether WM microstructural changes are a primary event, or secondary to GM atrophy [12].

Diffusion tensor imaging (DTI) and magnetization transfer (MT) imaging are among the most popular MRI techniques for assessing white matter changes, they are sensitive to micro-structural and metabolic changes, and therefore they might provide more accurate prognostic information than atrophy assessment on its own. DTI allows the estimation of a number of indices of microstructural integrity of white matter fiber tracts [13 - 14]. Among those, fractional anisotropy (FA) reflects the coherence of the orientation of water diffusion, and its variation is influenced by different factors including myelination, axon density, axonal

membrane integrity and axon diameter [15 - 16]. Mean diffusivity (MD) is determined by the density of physical obstructions to diffusion such as membranes, and quantifies the resultant distribution of water molecules between different cell compartments [16]. Higher MD values indicate increased diffusion which suggests tissue breakdown and increased brain water content [15]. As diverse pathological events can lead to similar changes in the observed FA and MD, it was proposed that parameters quantifying separately the diffusivity along and across WM tracts – namely axial diffusivity (ADif) and radial diffusivity (RDif) – can be more informative about the integrity of axons versus their surrounding myelin sheaths [17]. Increased RDif has been linked to loss of myelin in animal studies of experimentally induced myelin loss [17 - 19], while a decrease in ADif has been reported in both rodents and humans with axonal damage associated with axonal swelling, fragmentation and organelle accumulations [19 - 20].

Magnetization transfer (MT) imaging is based on the exchange of magnetization between protons in tissue water (liquid pool) and those bound to macromolecules (macromolecular pool). In particular, as some evidence suggests that molecules associated with myelin dominate the MT exchange process in WM, it is conceivable that this technique may provide information about myelin integrity. A simple way to quantify this effect is the MT ratio (MTR) [21], which has been extensively applied to the study of neurological conditions, including dementia. Previous investigations have demonstrated reductions of the MTR in the brain of patients with AD [22 - 23] and associations between MTR and measures of global cognitive impairment [24 - 26], suggesting that the MTR is sensitive to at least some of the pathological processes characterising AD. The MTR value, however, is the result of the combination of several more fundamental quantities, and it is known to be affected also by inflammation, T1 changes and pH [27]. Quantitative MT (qMT) [28] is an extension of MT imaging which attempts to overcome the limitation of MTR by quantifying the

physical properties that govern the MT process, including the relaxation rates of the pools, the exchange rate, and the relative size of the macromolecular pool. These parameters deliver information closely related to biological changes of WM and GM, and are therefore of potential interest in several neurological disorders. In particular, preliminary studies suggest that qMT might provide complementary information to that offered by other MRI techniques in the characterisation of neurodegenerative diseases, such as AD [23; 29 - 30].

Post-mortem studies [31] and animal studies [32 - 34] indicate that one of the parameters obtained from qMT, the relative size of the macromolecular pool, or F, is proportional to myelin content in WM [35], while preliminary studies indicates that another qMT parameter, namely the forward exchange rate, $RM_0^B$, might be more sensitive to AD pathology [29 - 30]. The interpretation of $RM_0^B$ is uncertain, as the exact mechanisms of MT are still unknown. Based on results obtained in the cortex of patients with Alzheimer's disease, it was suggested that it might reflect metabolic abnormalities [30], while recent reports indicate that it might be related to mild inflammatory changes [36 - 37].

Here, we combined DTI and qMT to provide a detailed examination of WM abnormalities in aMCI. Our primary aim was to identify tract-specific biomarkers obtained from DTI and qMT able to predict the conversion to AD in patients with aMCI over 1 year. In addition, secondary aims were a) to assess the microstructural damage of the WM tracts which were recently shown to be involved in AD pathophysiology [38] in patients with MCI; and b) to evaluate the relationship between qMT and DTI indices within those tracts. Our attention has focused on the cingulum and uncinate fasciculus, whose early involvement in AD pathology and relation to cognitive decline has been described by previous studies [9; 39]. The inferior longitudinal fasciculus has also been considered, given its proximity in the anterior part to the uncinate fasciculus.

## Materials and methods

### Subjects

A cohort of 43 patients with a diagnosis of probable AD [40], 34 patients with amnesic mild cognitive impairment (aMCI) [41] and 21 healthy controls (HC) were enrolled for this study. Patients were reviewed after 1 year, in order to assess whether they had converted to AD or remained stable. Patients were recruited from the specialist dementia clinic of the Catholic University of Rome (Rome, Italy). All patients had a typical clinical onset of AD, characterized by episodic memory deficits. The principal demographic and clinical characteristics of the participants are summarized in Table 1.

aMCI patients were identified according to current criteria [41]. They had to report a subjective memory impairment corroborated by an assistant and confirmed by performance below the normality cut off scores on at least one of the administered tests for episodic memory (see Table 2), and all MCI patients had not to fulfil the Diagnostic and Statistical Manual of Mental Disorders (DSM-V) criteria for the diagnosis of major neurocognitive disorders [42]. This criterion was confirmed by reporting normal scores at the Mini Mental State Examination (MMSE) [43 - 44] (Italian normality cut-off score > 23.8) [45] and at all tests of the neuropsychological battery assessing cognitive functions other than episodic memory (Table 2). Finally, the memory deficits observed in aMCI patients had to result in no or in a very mild impact on their daily living activities, as confirmed by their total Clinical Dementia Rating (CDR) score [46] which had not to exceed 0.5. None of the aMCI patients was either under anticholinesterase or neuroleptic medication. Patients with probable AD were diagnosed according to the clinical criteria established by the National Institute of Neurological and Communicative Disorders and Stroke Alzheimer's Disease and Related Disorders Association (NINCDSADRDA) [40].

HC were enrolled among patients' relatives and spouses. HC had to report no previous complaint suggestive of cognitive impairment, and they had to score within the range of normality at every administered neuropsychological test (Table 2).

All recruited subjects had to be right-handed, in order to reduce any potential source of variability due to hemispheric dominance. Major systemic, psychiatric and other neurological illnesses were carefully investigated and excluded in all the studied subjects. This research study was approved by the Ethics Committee of Santa Lucia Foundation, according to the principles expressed in the Declaration of Helsinki. Written informed consent (either from the participants or from their responsible guardians if incapable) were obtained before study initiation.

**Neuropsychological assessment**

All recruited patients underwent an extensive neuropsychological battery administered by two trained neuropsychologists on the same day of the MRI acquisition and at follow-up. Global cognitive function was assessed by means of the MMSE [43 - 44]. Patients underwent also a complete battery of tests specific for each cognitive domain: 1) Verbal episodic long-term memory: Immediate and Delayed recall of a 15-Word List [47], Short Story (Immediate and Delayed) [48]; 2) Visuo-spatial episodic long term memory: Immediate and Delayed recall of Complex Rey's Figure [48]; 3) short-term memory: Digit span forward and Corsi Block Tapping task forward [49]; 4) executive functions: Phonological Word Fluency [47]. Digit span backward and Corsi Block Tapping task backward [49] Language: Naming objects subtest of the BADA ("Batteria per l'Analisi dei Deficit Afasici", Italian for "Battery for the analysis of aphasic deficits"); and 5); Problem-solving: Raven's Coloured Progressive Matrices [47]; Praxis: Copy of drawings with and without landmarks [47]; Copy of Complex Rey's Figure [48]. For all administered tests, we

used the Italian normative data for score adjustment (gender, age, and education) and to define cut-off scores of normality, determined as the lower limit of the 95% tolerance interval for a confidence level of 95%. For each test, normative data are reported in the corresponding references. Group comparisons were estimated by seventeen one-way ANOVAs. To avoid the type-I error Bonferroni's correction was applied (statistical threshold for significance, p=0.003, $\alpha$= 0.05/16).

**MRI acquisition**

All MRI was obtained using a head-only 3T scanner (Siemens Magnetom Allegra, Siemens Medical Solutions, Erlangen, Germany), equipped with a circularly polarized transmit–receive coil. The maximum gradient strength is 40mTm$^{-1}$, with a maximum slew rate of 400T/m/s. The following sequences were obtained for each subject during a single scanning session: 1) dual-echo turbo spin echo (TSE) (TR=6190 ms, TE1=12 ms, TE2=109 ms, echo train length (ETL)=5; matrix=256x192; field of view (FOV)=230x172.5mm$^2$; 48 contiguous 3mm thick slices); 2) fluid attenuated inversion recovery (FLAIR) (TR=8170 ms, TE=96 ms, TI=2100 ms; ETL= 13; same FOV, matrix and number of slices as TSE); 3) morphological 3D T1-weighted magnetization prepared rapid acquisition gradient echo (MPRAGE) (TE=2.74 ms, TR=2500 ms, inversion time= 900 ms; flip angle=8; matrix=256x208x176; FOV=256x208x176mm$^3$); 4) diffusion weighted twice-refocused SE EPI (TR=170 ms, TE=85 ms, maximum b factor= 1000smm$^2$, isotropic resolution 2.3mm$^3$; matrix=9696; 60 slices), collecting seven images with no diffusion weighting (b0) and 61 images with diffusion gradients applied along 61 non-collinear directions [50]; 5) a series of 12 MT-weighted 3D fast low-angle shot (FLASH) sequences (TR=35 ms, TE=7.4, flip angle=7; matrix=128x96x28; FOV= 230x172.5x140mm$^3$), with various combinations of on-resonance equivalent flip angle and offset frequency ($\Delta$) of the Gaussian MT pulse (pulse duration= 15ms). The optimised set of sampling points matched that described in Cercignani

et al. [51]; 6) three 3D FLASH sequences with three different flip angles for mapping the observed T1 of the system (TR=15 ms, TE=4.8 ms, flip angle=5, 7, 15, respectively; same matrix and FOV as the MT-weighted FLASH); 7) three 3D FLASH sequences with near-180 flip angles for B1 mapping [52] (TR=28 ms, TE=4.8ms, flip angles=155, 180, 205, respectively; matrix=64x64x40, FOV=220x220x160mm$^3$); this sequence was collected along the sagittal plane, while all the other sequences were collected in the near-axial plane, with slices positioned to run parallel to a line that joins the most inferoanterior and inferoposterior parts of the corpus callosum (AC–PC line). The total scan time was approximately 60 minutes.

**MR images post-processing and analysis**

***Diffusion tensor MR imaging and probabilistic tractography***

Correction for eddy currents and the effects of involuntary movements on the DTI was by means of affine registration of each diffusion-weighted volume to the first non-diffusion weighted volume using FSL. Then FA, MD, RDif and ADif were computed from the diffusion tensor (DT) fitted with weighted linear least-square using Camino [53].

The WM tracts of interest were: the inferior longitudinal fasciculus (ILF), the interior (ventral) and superior (dorsal) cingulum bundles (infCi and SupCi), and the uncinated fasciculus (UF). The tracts were reconstructed in native space for all participants, using multi-fiber probabilistic tractography. Tractography was carried out using 10000 iterations of the probabilistic index of connectivity (PICo) algorithm applied to fibre orientation distribution functions estimated with persistent angular structure (PAS) MRI. Seed and way points to reconstruct the tracts of interest were defined on each subject's colour coded map according to published guidelines. Anatomical images were used to increased confidence in seed-point selection. The criteria used to select seed and way points for each tract are presented as Supplementary material.

***Quantitative MT analysis***

For all the subjects, FLASH images from sequence 7 were reformatted to the axial plane. Next, in order to compensate for involuntary motion, all images obtained from sequences 5 (MT FLASH), 6 (T1-mapping FLASH) and 7 (reformatted B1-mapping FLASH) were affine-registered using FLIRT [54 – 55] to match the $15^0$ flip-angle scan obtained with sequence 6. B1 maps were computed according to Dowell and Tofts, [52] and T1 maps were calculated by fitting the theoretical spoiled gradient echo signal equation [56] as a function of the flip angle (after B1-correction) to the signal measured by sequence 6 [57]. A detailed description of the processing is given elsewhere [51]. For MT modelling, we adopted here Ramani's signal equation [58] a modification of Henkelman's model [28] for in vivo applications, where the continuous wave power equivalent (CWPE) approximation is used. As described in detail elsewhere [51; 59] quantitative MT parameters were estimated on a voxel-by-voxel basis by fitting the model equation of the MT-weighted signal to the data from sequence 5 using the Levenberg– Marquardt method, as implemented in Numerical Recipes [60]. The absorption lineshape of the macromolecular pool was modelled with a super-Lorentzian [61]. The longitudinal relaxation rate of the macromolecular pool, $RM_0^B$, was set arbitrarily to 1 $s^{-1}$ and kept fixed during the fitting, as in previous quantitative MT experiments [28; 62; 63]. The fitting yielded maps of F and $RM_0^B$.

***Extraction of Tract-specific Indices***

For every subject, the spatial transformation matching the DTI scan to the MT-weighted scans was then computed by affine registration and followed by nonlinear registration (see FLIRT and FNIRT, http:// www.fmrib.ox.ac.uk/fsl/fsl/list.html). The non-linear step was added to compensate for EPI geometric distortions. The transformations were then applied to the maps defining the WM tracts which were used to compute the tract mean F, $RM_0^B$. The tract average FA, MD, ADif, RDif were also computed.

**Statistical analysis**

Statistical analyses were performed using SPSS 15.0 for Windows (SPSS Inc, USA). Age and gender were compared between groups using a one-way ANOVA and a $\chi^2$-test, respectively. Between-group comparisons of tract volumes, mean qMT (F and $RM_0^B$) and DTI (FA, MD, ADif and RDif) parameters were performed using a one-way ANOVA, Tukey tests were used to assess group differences (post-hoc analyses). The significance level for the ANOVAs was set to p=0.008, after Bonferroni's correction ($\alpha$=0.05/6). The presence of any association between DTI and qMT parameters was assessed using the Pearson correlation. The significance level was set after Bonferroni's correction (p=0.015; $\alpha$= 0.05/4).

**Results**

After 1 year, 17 aMCI remained stable ($MCI_{stable}$) and 17 converted to probable AD ($MCI_{converters}$).Table 1 summarizes the demographical and clinical characteristics of all the patients and HC, together with the statistical differences. A significant difference in age was detected between HC and AD, and between $MCI_{converters}$ and AD ($p< 0.05$ in both cases). Moreover, on average, HC had received more years of education when compared to AD ($p< 0.01$). Both age and years of education were introduced in the statistical analysis as variables of no interest. As expected, the baseline MMSE scores were significantly higher in HC, $MCI_{converters}$ and $MCI_{stable}$ when compared to AD, and significantly higher in $MCI_{converters}$ when compared to $MCI_{stable.}$ No other differences were found between $MCI_{converters}$ and $MCI_{stable}$.

***Neuropsychological and behavioral assessments***

Neuropsychological data for the group of AD and MCI patients and HC volunteers are summarized in Table 2. As expected, the performance of AD patients was significantly poorer than HC in all cognitive domains. Both MCI groups performed worse than HC in immediate and delayed recall of the 15-word list, and delayed recall of short story test.

$MCI_{converters}$ but not $MCI_{stable}$ performed worse than HC in immediate and delayed recall of Complex Rey's figure, verbal digit span forward and backward, modified card sorting test and Raven's colored progressive matrices. Conversely, when compared to AD, both $MCI_{converters}$ but not $MCI_{stable}$ reported better performance in immediate recall of 15 words, delayed recall of short story, world fluency test, copy of drawings with landmarks. $MCI_{stable}$ but not $MCI_{converters}$ performed better than AD in delayed recall of 15 words, Corsi span, digit span backward, Raven's colored progressive matrices and copy of drawings. When compared to each other, $MCI_{converters}$ performed worse than $MCI_{stable}$ at the delayed recall of 15 word list and modified card sorting test (see Table 2).

***DTI results***

We first investigated the presence of between-group differences in the volume of WM tracts, in order to exclude that difference in DTI and qMT indices were affected by partial volume related to the overall atrophy rather than to mictrostructural damage. A one-way ANOVA reported significant differences in the volume of infCI (for both left and right $p<0.005$) and ILF (for both left and right $p=0.05$) in AD and $MCI_{converters}$ reported reduced volume in left infCI when compared to HC, whereas only $MCI_{converters}$ reported reduced volume in right infCi when compared to HC (all $p< 0.005$). $MCI_{stable}$ reported reduced volume in left ILF when compared to HC ($p<0.05$). Volumes of infCi and ILF have been introduced as covariates of no interest in the subsequent analysis.

Significant differences were found in all DTI measures when comparing the three groups (Figures 1 and 2). Overall, AD patients presented changes in all DTI parameters (but FA) in all tracts when compared to HC. Several differences were found also when comparing the two subgroups of MCI ($MCI_{converters}$ and $MCI_{stable}$) to HC, as shown in Figure 1 (FA and MD) and Figure 2 (RDif and ADif). The only significant differences between $MCI_{converters}$ and $MCI_{stable}$ were found with FA of the supCi.

***qMT results***

Among the three groups, significant differences were found only with $RM_0^B$. When compared to HC, AD patients reported lower $RM_0^B$ in left ILF, bilateral infCI and left supCI (all $p<0.005$). Similarily, $MCI_{converters}$ (but not $MCI_{stable}$) had lower levels of $RM_0^B$ in left ILF, bilateral infCi and right UF when compared to HC. A difference between $MCI_{stable}$ and AD patients emerged in right infCi. When directly comparing $MCI_{converters}$ to $MCI_{stable,}$ the former group reported lower $RM_0^B$ in right UF (Figure3). No significant results emerged when considering F values.

***Correlation between DTI and qMT metrics***

Table 3 summarizes the correlations between DTI and qMT matrices in the WM tracts of interest. MD and $RM_0^B$ values were negatively correlated in almost all tracts (except right ILF and UF left). MD correlated negatively also with F values in supCI left and UF left. Similarly, in all tracts (but left ILF), we observed a negative correlation between RDif and $RM_0^B$ parameter. A negative correlation was evident between RDif and F in left UF. As regards ADif, a negative correlation was evident with $RM_0^B$ values of the bilateral inferior cingulum, whereas no correlation was evident with F values. Finally, a positive correlation was observed between FA and $RM_0^B$ values in bilateral ILF and F values in left UF. It is interesting to observe that most of these correlations, albeit significant, were modest ($R<0.5$).

**Discussion**

This study sought to identify alterations in white matter tracts, measurable in the brain of MCI patients up to a year before they converted to AD. In order to capture the full extent of WM changes in aMCI and AD, we considered both DTI and qMT indices in the major tracts involved in AD: inferior longitudinal fasciculus, inferior and superior cingulum and uncinate fasciculus.

A number of major results emerged. First, we identified 2 potential biomarkes of conversion to AD: FA in supCi and $RM_0^B$ in UF, which can differentiate $MCI_{converters}$ from $MCI_{stable}$ already at baseline.

Both UF and the cingulum are known to be involved in AD pathology [39; 65 - 65]. The UF is one of principal pathways of connection between temporal and frontal lobes, and therefore damage to this tract might explain some aspects of memory impairment, such as those related with encoding and retrieval of new material [66 - 67]. Previous studies have also postulated a role for the UF as predictor of the conversion from aMCI to AD [68], and this tract has been linked to memory and emotional recognition alterations in aMCI [69]. Interestingly, a previous study from our group showed that damage to the UF, by means of reduced FA, was measurable in patients with AD, but not in those with MCI [39].

The cingulum bundle is the major median associative WM fasciculus reciprocally connecting various frontal, temporal, and parietal regions. It is part of both, the executive control and default mode networks, which are responsible for executive function, memory and other cognitive functions [70]. The damage in the cingulum has been found to correlate with measures of cognitive impairment [71], and we have previously shown that it correlates with atrophy of the nearby GM structures [9]. It is therefore unsurprising that measures of microstructural damage to this tract can be sensitive to the conversion to AD.

In line with these findings, we show that, at baseline, $MCI_{converters}$ already show some microstructural differences compared to HC, which resemble those exhibited by AD patients. This result matches what has already been shown for GM atrophy [5], i.e. that MCI who are about to convert to AD will show a degree of tissue damage comparable to AD patients prior to conversion, while such damage is undetectable in those MCI patients who remain stable. Interestingly, these WM abnormalities can be detected by the DTI indices MD, RDif and

ADif, and by the qMT parameters $RM_0^B$, but not by FA or F. This probably indicates a pathological substrate of inflammatory nature, with no frank demyelination or tissue loss.

$MCI_{stable}$ only show signs of mild microstructural damage when compared to HC, evidenced by an increase in ADif in infCi and UF. The interpretation of these findings is highly speculative, as we cannot be sure whether this group of patient will ever develop a form of dementia. However, if we were to hypothesise that they represent a group of very early AD patients, the focal involvement of these tracts fits with the frequently reported (and above discussed) evidence of microstructural damage to the cingulum and the UF in AD patients [9; 39] and MCI [68; 72].

The main novelty of this paper is in the combination of qMT and DTI parameters, and in the multi-parametric evaluation of the major WM tracts. The potential role of qMT in the evaluation of patients with AD was highlighted by 3 previous papers [23; 29 - 30]. Here we extended the analysis to the population of MCI individuals. Our data confirm the sensitivity of the parameter $RM_0^B$ in detecting pathophysiological changes in AD [30]. In contrast to our initial hypothesis, F, which has been linked to myelin damage, was not sensitive to alterations in WM tracts, while the DTI parameter RDif, believed to also reflect myelin damage, showed some abnormalities in $MCI_{converters}$. The lack of correlation between the two parameters, although unexpected, has been already described in other studies [32; 73]. The reason for such a discrepancy might be explained by the underlying physical principles between the two imaging techniques [33; 73], where DTI indices reflect mainly the directionality of WM fibres whereas qMT parameters reflects tissue composition rather than spatial organization. An overall increase in diffusivity (which can be associated with tissue loss and inflammation) would also result in an increase of RDif, with no associated change in F.

In support of this speculation, values of RDif mostly correlated with values of $RM_0^B$ in almost all tracts (but ILF right), suggesting that the two parameters might reflect similar – or highly linked - structural contributions to WM integrity in this sample. An intriguing speculation on the clinical relevance of the parameter $RM_0^B$ in AD has been put forward in a previous study from our group [30], suggesting that this parameter might reflect some metabolic information [74] and supporting the hypothesis that mitochondrial dysfunction might play a relevant role in the pathophysiology of AD [75]. Whereas this still remains a purely speculative explanation, it is worth noting that mitochondrial dysfunction contributes to white matter demyelination in multiple sclerosis [76 - 77], suggesting a similar mechanism in the WM damage in AD and providing a possible explanation of the correlation between RDif and $RM_0^B$ indices in our study. Of note, changes in $RM_0^B$ of the insular cortex were recently shown in experimentally induced systemic inflammation, and were interpreted as localized increase in metabolically-active macromolecules [36]. This might also explain why in our study different indices of WM microsturcutre are more sensitive to the damage in different tracts. Whilst part of it might be due to the different fibre architecture in the various tracts [78], other might be explained by the specific pathological process occurring in specific tracts. For example, UF carries cholinergic fibres from the basal nucleus of Meynert innervating frontal and temporal regions [79]. The integrity of cholinergic system is highly vulnerable to metabolic state, suggesting again that $RM_0^B$ (the most sensitive marker in spotting WM damage in UF when comparing $MCI_{converters}$ and $MCI_{stable}$) might be eloquent of underlying metabolic processes. In fact, the hypothesis of a cholinergic deficit in AD and its pathofisiological consequences have a long history. It is known that an impairment of cholinergic transmission one of the features of neurodegeneration which occurs early in AD, and the loss of cholinergic neurons and projections is well described in the AD pathology [80]. Albeit these hypotheses are intriguing, further interpretations are beyond the scope of

this study and future research is needed to investigate the clinical relevance of qMT parameters extracted from WM tracts.

In conclusion, our study reveals that qMT and DTI indices extracted from tractography are efficient in spotting the WM microstructural damage and are valid biomarkers of the conversion from MCI to AD. Combined with neuropsychological evaluation, the complementary information from these markers could be applied in future for the development of multivariate tools for the early identification of patients who are likely to benefit from therapeutic intervention.

**References**


[1] Mitchell AJ, Shiri-Feshki M (2009) Rate of progression of mild cognitive impairment to dementia-meta-analysis of 41 robust inception cohort studies. *Acta Psychiatrica Scandinavica* **119**, 252–265.

[2] Perri R, Serra L, Carlesimo GA, Caltagirone C (2007) Amnestic mild cognitive impairment: difference of memory profile in subjects who converted or did not convert to Alzheimer's disease. *Neuropsychology* **21**, 549-558.

[3] Mufson EJ, Binder L, Counts SE, DeKosky ST, deTolledo-Morrell L, Ginsberg, SD, Scheff, SW (2012) Mild Cognitive Impairment: Pathology and mechanisms. *Acta Neuropathologica* **123**, 13–30. 10.1007/s00401-011-0884-1

[4] Petersen RC, Doody R, Kurz A, Mohs RC, Morris JC, Rabins PV, Ritchie K, Rossor M, Thal L, Winblad B (2001) Current concepts in mild cognitive impairment. *Arch Neurol* **58**, 1985-1992.

[5] Bozzali M, Filippi M, Magnani G, Cercignani M, Franceschi M, Schiatti E, Castiglioni S, Mossini R, Falautano M, Scotti G, Comi G, Falini A (2006) The contribution of voxel-based morphometry in staging patients with mild cognitive impairment. *Neurology* **67**, 453–460.

[6] Devanand DP, Liu X, Tabert MH, Pradhaban G, Cuasay K, Bell K, de Leon MJ, Doty RL, Stern Y, Pelton GH (2008) Combining early markers strongly predicts conversion from mild cognitive impairment to Alzheimer's disease. *Biol Psychiatry* **64**, 871–879.

[7] Bozzali M, Padovani A, Caltagirone C, Borroni B (2011) Regional grey matter loss and brain disconnection across Alzheimer disease evolution. *Curr Med Chem* **18**, 2452-8.

[8] Bozzali M, Cherubini A (2007) Diffusion tensor MRI to investigate dementias: a brief review. *Magn Reson Imaging* **25**, 969–977.

[9] Bozzali M, Giulietti G, Basile B, Serra L, Spanò B, Perri R, Giubilei F, Marra C, Caltagirone C, Cercignani M (2012) Damage to the cingulum contributes to Alzheimer's disease pathophysiology by deafferentation mechanism. *Hum Brain Mapp* **33**, 1295-308.

[10] Bartzokis (2011) Alzheimer's disease as homeostatic responses to age-related myelin breakdown. *Neurobiol Aging* **32**, 1341-71.

[11] Gold BT, Johnson NF, Powell DK, Smith CD (2012) White matter integrity and vulnerability to Alzheimer's disease: preliminary findings and future directions. *Biochim Biophys Acta* **1822**, 416–22.

[12] Pierpaoli C, Barnett A, Pajevic S, Chen R, Penix LR, Virta A, Basser P (2001) Water diffusion changes in Wallerian degeneration and their dependence on WM architecture. *Neuroimage* **13**, 1174–1185.

[13] Le Bihan D, Mangin JF, Poupon C, Clark CA, Pappata S, Molko N, Chabriat H (2001). Diffusion tensor imaging: concepts and applications. *J Magn Reson Imaging* **13**, 534–546.

[14] Sundgren PC, Dong Q, Gómez-Hassan D, Mukherji SK, Maly P, Welsh R (2004). Diffusion tensor imaging of the brain: review of clinical applications. *Neuroradiology* **46**, 339–350.

[15] Pierpaoli C and Basser PJ (1996). Toward a quantitative assessment of diffusion anisotropy, *Magn Reson Med* **36**, 893–906.

[16] Beaulieu C (2002) The basis of anisotropic water diffusion in the nervous system–a technical review. *NMR Biomed* **15**, 435–455.

[17] Song SK, Sun SW, Ramsbottom MJ, Chang C, Russell J, Cross AH (2002) Dysmyelination revealed through MRI as increased radial (but unchanged axial) diffusion of water. *Neuroimage* **17,** 1429–1436.

[18] Song SK, Yoshino J, Le TQ, Lin SJ, Sun SW, Cross AH (2005). Armstrong R.C. Demyelination increases radial diffusivity in corpus callosum of mouse brain. *Neuroimage* **26**, 132–140.

[19] Sun SW, Liang HF, Trinkaus K, Cross AH, Armstrong RC, Song SK (2006). Noninvasive detection of cuprizone induced axonal damage and demyelination in the mouse corpus callosum. *Magn Reson Med* **55**, 302–308.

[20] Concha L, Gross DW, Wheatley BM, Beaulieu C (2006). Diffusion tensor imaging of time-dependent axonal and myelin degradation after corpus callosotomy in epilepsy patients. *Neuroimage* **32**, 1090–1099.

[21] Dousset V, Brochet B, Vital A, Gross C, Benazzouz A, Boullerne A, Bidabe AM, Gin AM, Caille JM (1995) Lysolecithin-induced demyelination in primates: preliminary in vivo study with MR and magnetization transfer. *AJNR Am J Neuroradiol* **16**, 225-231.

[22] Bozzali M, Franceschi M, Falini A, Pontesilli S, Cercignani M, Magnani G, Scotti G, Comi G, Filippi M, (2001) Quantification of tissue damage in AD using diffusion tensor and magnetization transfer MRI. *Neurology* **57**, 1135–1137.

[23] Ridha BH, Tozer DJ, Symms MR, Stockton KC, Lewis EB, Siddique MM, MacManus DG, Rossor MN, Fox NC, Tofts PS (2007) Quantitative magnetization transfer imaging in Alzheimer disease. *Radiology* **244,** 832–37.

[24] Fornari E, Maeder P, Meuli R, Ghika J, Knyazeva MG (2010) Demyelination of superficial white matter in early Alzheimer's disease: a magnetization transfer imaging study. *Neurobiol Aging* **33**, 428.

[25] Hanyu H, Asano T, Iwamoto T, Takasaki M, Shindo H, Abe K (2000) Magnetization transfer measurements of the hippocampus in patients with Alzheimer's disease, vascular dementia, and other types of dementia. *AJNR Am J Neuroradiol* **21**, 1235–1242.

[26] Lee KY, Kim TK, Park M, Ko S, Song IC, Cho IH (2004) Age-related changes in conventional and magnetization transfer MR imaging in elderly people: comparison with neurocognitive performance. *Korean J Radiol* **5**, 96–101.

[27] Henkelman RM, Stanisz GJ, Graham SJ (2001) Magnetization transfer in MRI: a review. *NMR in Biomedicine* **14,** 57–64.

[28] Henkelman RM, Huang X, Xiang QS, Stanisz GJ, Swanson SD, Bronskill MJ (1993) Quantitative interpretation of magnetization transfer. *Magn Reson Med* **29**, 759–766.

[29] Kiefer C, Brockhaus L, Cattapan-Ludewig K, Ballinari P, Burren Y, Schroth G, Wiest R (2009) Multi-parametric classification of Alzheimer's disease and mild cognitive impairment: the impact of quantitative magnetization transfer MRimaging. *Neuroimage* **48,** 657-67.

[30] Giulietti G, Bozzali M, Figura V, Spanò B, Perri R, Marra C, Lacidogna G, Giubilei F, Caltagirone C, Cercignani M (2012) Quantitative magnetization transfer provides information complementary to grey matter atrophy in Alzheimer’s disease brains. *NeuroImage* **59**, 1114–1122.

[31] Schmierer K, Tozer DJ, Scaravilli F, Altmann DR, Barker GJ, Tofts PS, Miller DH (2007) Quantitative magnetization transfer imaging in postmortem multiple sclerosis brain. *J Magn Reson Imaging* **26**, 41–51.

[32] Ou X, Sun SW, Liang HF, Song SK, Gochberg DF (2009) Quantitative magnetization transfer measured pool-size ratio reflects optic nerve myelin content in ex vivo mice. *Magn Reson Med* **61**, 364–371.

[33] Ou X, Sun SW, Liang HF, Song SK, Gochberg DF (2009) The MT pool size ratio and the DTI radial diffusivity may reflect the myelination in shiverer and control mice. *NMR Biomed* **22**, 480–487.

[34] Turati L, Moscatelli M, Mastropietro A, Dowell NG, Zucca I, Erbetta A, Cordiglieri C, Brenna G, Bianchi B, Mantegazza R, Cercignani M, Baggi F, Minati L (2015) In vivo quantitative magnetization transfer imaging correlates with histology during de- and remyelination in cuprizone-treated mice. *NMR Biomed* **28**, 327-37.

[35] Janve VA, Zu Z, Yao SY, Li K, Zhang FL, Wilson KJ, Ou X, Does MD, Subramaniam S, Gochberg DF (2013) The radial diffusivity and magnetization transfer pool size ratio are sensitive markers for demyelination in a rat model of type III multiple sclerosis (MS) lesions. *Neuroimage* **74**, 298-305.

[36] Harrison NA, Cooper E, Dowell NG, Keramida G, Voon V, Critchley HD, Cercignani M (2014) Quantitative Magnetization Transfer Imaging as a Biomarker for Effects of Systemic Inflammation on the Brain. *Biol Psychiatry* **78**, 49-57.

[38] Agosta F, Pievani M, Sala S, Geroldi C, Galluzzi S, Frisoni GB, Filippi M (2011) White matter damage in Alzheimer disease and its relationship to gray matter atrophy. *Radiology* **258**, 853-63.

[39] Serra L, Cercignani M, Basile B, Spanò B, Perri R, Fadda L, Marra C, Giubilei F, Caltagirone C, Bozzali M (2012) White matter damage along the uncinate fasciculus contributes to cognitive decline in AD and DLB. *Curr Alzheimer Res* **9**, 326-33.

[40] McKhann GM, Knopman DS, Chertkow H, Hyman BT, Jack CR Jr, Kawas CH, Klunk WE, Koroshetz WJ, Manly JJ, Mayeux R, Mohs RC, Morris JC, Rossor MN, Scheltens P, Carrillo

MC, Thies B, Weintraub S, Phelps CH (2011) The diagnosis of dementia due to Alzheimer's disease: recommendations from the National Institute on Aging-Alzheimer's Association workgroups on diagnostic guidelines for Alzheimer's disease. *Alzheimers Dement* **7**, 263-269.

[41] Petersen RC, Caracciolo B, Brayne C, Gauthier S, Jelic V, Fratiglioni L (2014) Mild cognitive impairment: a concept in evolution. *J Intern Med* **275**, 214-228.

[42] American Psychiatric Association (2000) DSM-IV-TR. Diagnostic and Statistical Manual of Mental Disorder, Fourth Edition, Text Revision, Milano.

[43] Folstein MF, Folstein SE, McHugh PR (1975) "Mini-mental state". A practical method for grading the cognitive state of patients for the clinician. *J Psychiatr Res* **12**, 189-198.

[44] Measso G, Cavartezan F, Zappal`a G, Lebowitz DB, Crook TH, Pirozzolo FJ, Amaducci L, Massari D, Grigoletto F (1993) The Mini Mental State Examination: Normative study of a random sample of Italian population. *Dev Neuropsychol* **9**, 77-85.

[45] Magni E, Binetti G, Padovani A, Cappa SF, Bianchetti A, Trabucchi M (1996) The Mini-Mental State Examination in Alzheimer's disease and multi-infarct dementia. *Int Psychogeriatr* **8**, 127-134.

[46] Hughes CP, Berg L, Danziger WL, Coben LA, Martin R (1982) A new clinical scale for the staging of dementia. *Br J Psychiatry* **40**, 566-572.

[47] Carlesimo GA, Caltagirone C, Gainotti G, (1996) The mental Deterioration Battery: normative data, diagnostic reliability and qualitative analyses of cognitive impairment. The group of the Standardization of the Mental Deterioration Battery. *Eur Neurol* **36**, 378-384.

[48] Carlesimo GA, Buccione I, Fadda L, Graceffa A, Mauri M, Lo russo S, Bevilacqua G, Caltagirone C, (2002) Standardizzazione di due test di memoria per uso clinico: Breve Racconto e Figura di Rey. *Nuova Rivista di Neurologia* **12**, 1-13.

[49] Monaco M, Costa A, Caltagirone C, Carlesimo GA (2013) Forward and backward span for verbal and visuo-spatial data: standardization and normative data from an Italian adult population. *Neurol Sci* **34**, 749-54.

[50] Jones DK, Horsfield MA, Simmons A (1999) Optimal strategies for measuring diffusion in anisotropic systems by magnetic resonance imaging. *Magn Reson Med* **42**, 515–525.

[51] Cercignani M, Basile B, Spanò B, Comanducci G, Fasano F, Caltagirone C, Nocentini U, Bozzali M (2009) Investigation of quantitative magnetisation transfer parameters of lesions and normal appearing white matter in multiple sclerosis. *NMR Biomed* **22**, 646–653.

[52] Dowell NG, Tofts PS (2007) Fast, accurate, and precise mapping of the RF field in vivo using the 180 degrees signal null. *Magn Reson Med* **58**, 622–630.

[53] http://camino.cs.ucl.ac.uk/

[54] Jenkinson M, Smith S (2001) A global optimisation method for robust affine registration of brain images. *Med Image Anal* **5**, 143–156.

[55] Jenkinson M, Bannister P, Brady M, Smith S (2002) Improved optimization for the robust and accurate linear registration and motion correction of brain images. *Neuroimage* **17**, 825–841.

[56] Ernst T, Anderson W (1966) Application of Fourier transform spectroscopy to magnetic resonance. *Rev Sci Instrum* **37**, 93–102.

[57] Dowell NG, Cooper EA, Tibble J, Voon V, Critchley HD, Cercignani M, Harrison NA (2016) Acute Changes in Striatal Microstructure Predict the Development of Interferon-Alpha Induced Fatigue. *Biol Psychiatry* **79,** 320-8.

[57] Venkatesan R, Lin W, Haacke EM (1998) Accurate determination of spin-density and T1 in the presence of RF-field inhomogeneities and flip-angle miscalibration. *Magn Reson Med* **40**, 592–602.

[58] Cercignani M, Alexander DC (2006) Optimal acquisition schemes for in vivo quantitative magnetization transfer MRI. *Magn Reson Med* **56**, 803–810.

[59] Cercignani M, Symms MR, Schmierer K, Boulby PA, Tozer DJ, Ron M, Tofts PS, Barker GJ (2005) Three-dimensional quantitative magnetisation transfer imaging of the human brain. *Neuroimage* **27**, 436–441.

[60] Press WH, Teukolsky SA, Vettering WT, Flannery BP (1992) Numerical recipes in C. Cambridge University Press, Cambridge.

[61] Morrison C, Stanisz G, Henkelman RM (1995) Modeling magnetization transfer for biological-like systems using a semi-solid pool with a super-Lorentzian lineshape and dipolar reservoir. *J Magn Reson B* **108**, 103–113.

[62] Tozer D, Ramani A, Barker GJ, Davies GR, Miller DH, Tofts PS (2003) Quantitative magnetization transfer mapping of bound protons in multiple sclerosis. *Magn Reson Med* **50**, 83–91.

[63] Narayanan S, Francis SJ, Sled JG, Santos AC, Antel S, Levesque I, Brass S, Lapierre Y, Sappey-Marinier D, Pike GB, Arnold DL (2006) Axonal injury in the cerebral normal-appearing white matter of patients with multiple sclerosis is related to concurrent demyelination in lesions but not to concurrent demyelination in normal-appearing white matter. *Neuroimage* **29**, 637–642.

[64] Bosch B, Arenaza-Urquijo EM, Rami L, Sala-Llonch R, Junqué C, Solé-Padullés C, Peña-Gómez C, Bargalló N, Molinuevo JL, Bartrés-Faz D (2012) Multiple DTI index analysis in normal aging, amnestic MCI and AD. Relationship with neuropsychological performance. *Neurobiol Aging* **33**, 61-74.

[65] Stebbins GT, Murphy CM (2009) Diffusion tensor imaging in Alzheimer's disease and mild cognitive impairment. *Behav Neurol* **21**, 39-49.

[66] Horel JA (1978) The neuroanatomy of amnesia. A critique of the hippocampal memory hypothesis. *Brain* **101**, 403-445.

[67] Levine B, Black SE, Cabeza R, Sinden M, McIntosh AR, Toth JP, Tulving E, Stuss DT (1998) Episodic memory and the self in a case of isolated retrograde amnesia. *Brain* **121**, 1951-73.

[68] Hiyoshi-Taniguchi K, Oishi N, Namiki C, Miyata J, Murai T, Cichocki A, Fukuyama H (2015) The Uncinate Fasciculus as a Predictor of Conversion from aMCI to Alzheimer Disease. *J Neuroimaging* **25**, 748-53.

[69] Fujie S, Namiki C, Nishi H, Yamada M, Miyata J, Sakata D, Sawamoto N, Fukuyama H, Hayashi T, Murai T (2008) The role of the uncinate fasciculus in memory and emotional recognition in amnestic mild cognitive impairment. *Dement Geriatr Cogn Disord* **26(5),** 432-9.

[70] van den Heuvel M, Mandl R, Luigjes J, Hulshoff Pol H (2008) Microstructural organization of the cingulum tract and the level of default mode functional connectivity. *J Neurosci* **28**, 10844–10851.

[71] Xie S, Xiao JX, Wang YH, Wu HK, Gong GL, Jiang XX (2005) Evaluation of bilateral cingulum with tractography in patients with Alzheimer's disease. *Neuroreport* **16**, 1275–1278.

[72] Ito K, Sasaki M, Takahashi J, Uwano I, Yamashita F, Higuchi S, Goodwin J, Harada T, Kudo K, Terayama Y (2015) Detection of early changes in the parahippocampal and posterior cingulum bundles during mild cognitive impairment by using high-resolution multi-parametric diffusion tensor imaging. *Psychiatry Res* **231**, 346-52.

[73] Underhill HR, Yuan C, Yarnykh VL (2009) Direct quantitative comparison between cross-relaxation imaging and diffusion tensor imaging of the human brain at 3.0 T. *Neuroimage* **47**, 1568-1578.

[74] Louie EA, Gochberg DF, Does MD, Damon BM (2009). Transverse relaxation and magnetization transfer in skeletal muscle: effect of pH. *Magn Reson Med* **61**, 560–569.

[75] Moreira PI, Carvalho C, Zhu X, Smith MA, Perry G (2010). Mitochondrial dysfunction is a trigger of Alzheimer's disease pathophysiology. *Biochim Biophys Acta* **1802**, 2–10.

[76] Witte ME, Mahad DJ, Lassmann H, van Horssen J (2014) Mitochondrial dysfunction contributes to neurodegeneration in multiple sclerosis. *Trends Mol Med* **20**, 179-187.

[77] Carvalho KS (2013) Mitochondrial dysfunction in demyelinating diseases. *Semin Pediatr Neurol* **20**, 194-201.

[78] De Santis S, Drakesmith M, Bells S, Assaf Y, Jones DK (2014). Why diffusion tensor MRI does well only some of the time: variance and covariance of white matter tissue microstructure attributes in the living human brain. *Neuroimage* **89**, 35-44.

[79] Selden NR, Gitelman DR, Salamon-Murayama N, Parrish TB, Mesulam MM (1998) Trajectories of cholinergic pathways within cerebral hemispheres of the human brain. *Brain* **121**, 2249–2257.

[80] Francis PT, Palmer AM, Snape M, Wilcock GK (1999) The cholinergic hypothesis of Alzheimer's disease: a review of progress. *J Neurol Neurosurg Psychiatry* **66**, 137-47.

**Figure 1.**

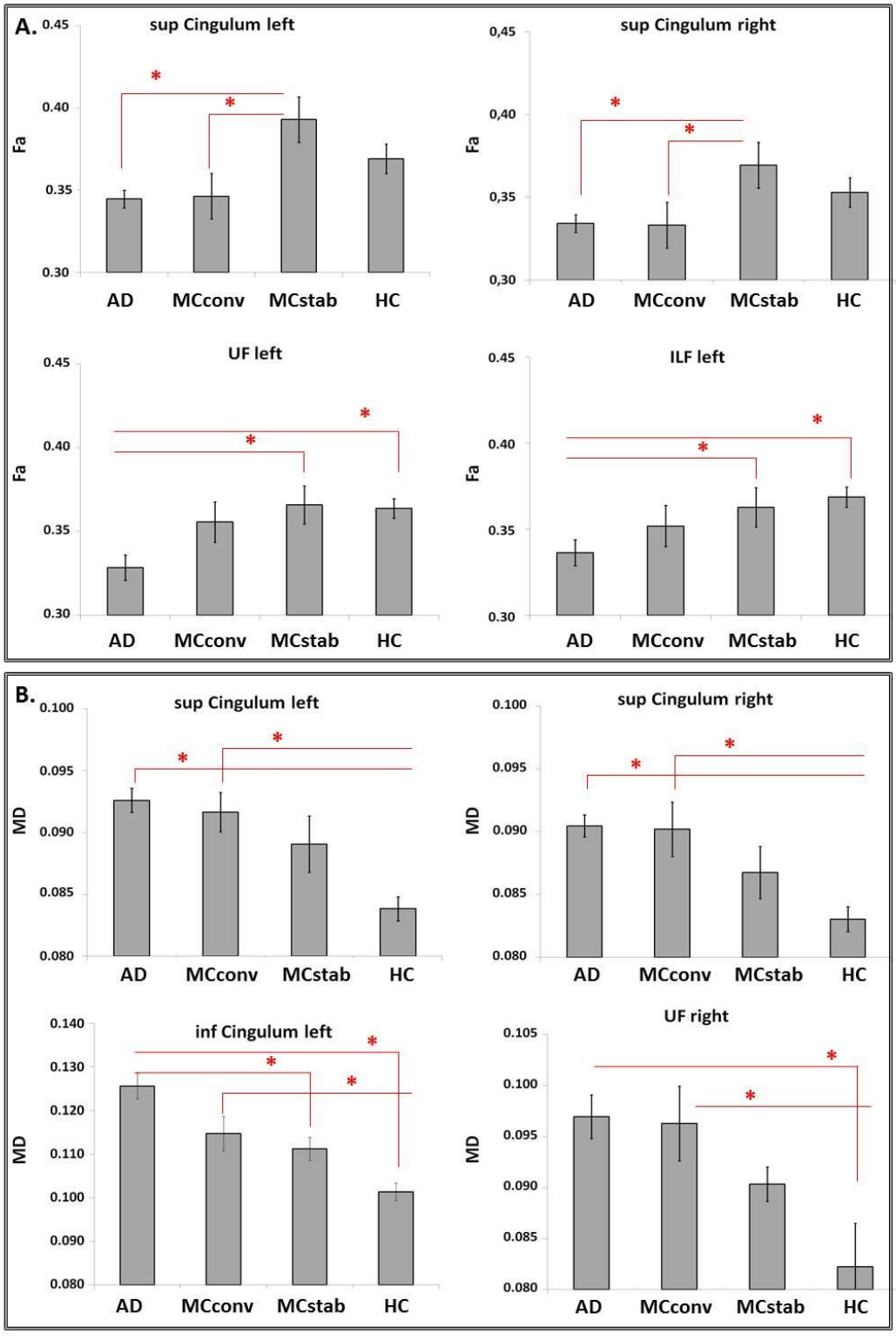


**Figure 1.** Average group FA (A) and MD (B) values in the tracts of interest. Data are reported only for tracts that showed at least one between group significant difference. Differences between AD and HC are widespread. By contrast, only FA of supCI differentiated MCIconverters from MCIstable already at baseline. Abbreviations: AD= Alzheimer's disease; HC = healthy controls; MCIconv = MCI that converted to AD at follow-up; MCIstab = MCI

that remained stable (did not convert to AD) at follow-up; Fa= franctional anisotropy; MD= mean diffusivity; sup= superior; inf= inferior; UF= uncinated fasciculus; ILF= inferior longitudinal fasciculus.

**Figure 2.**

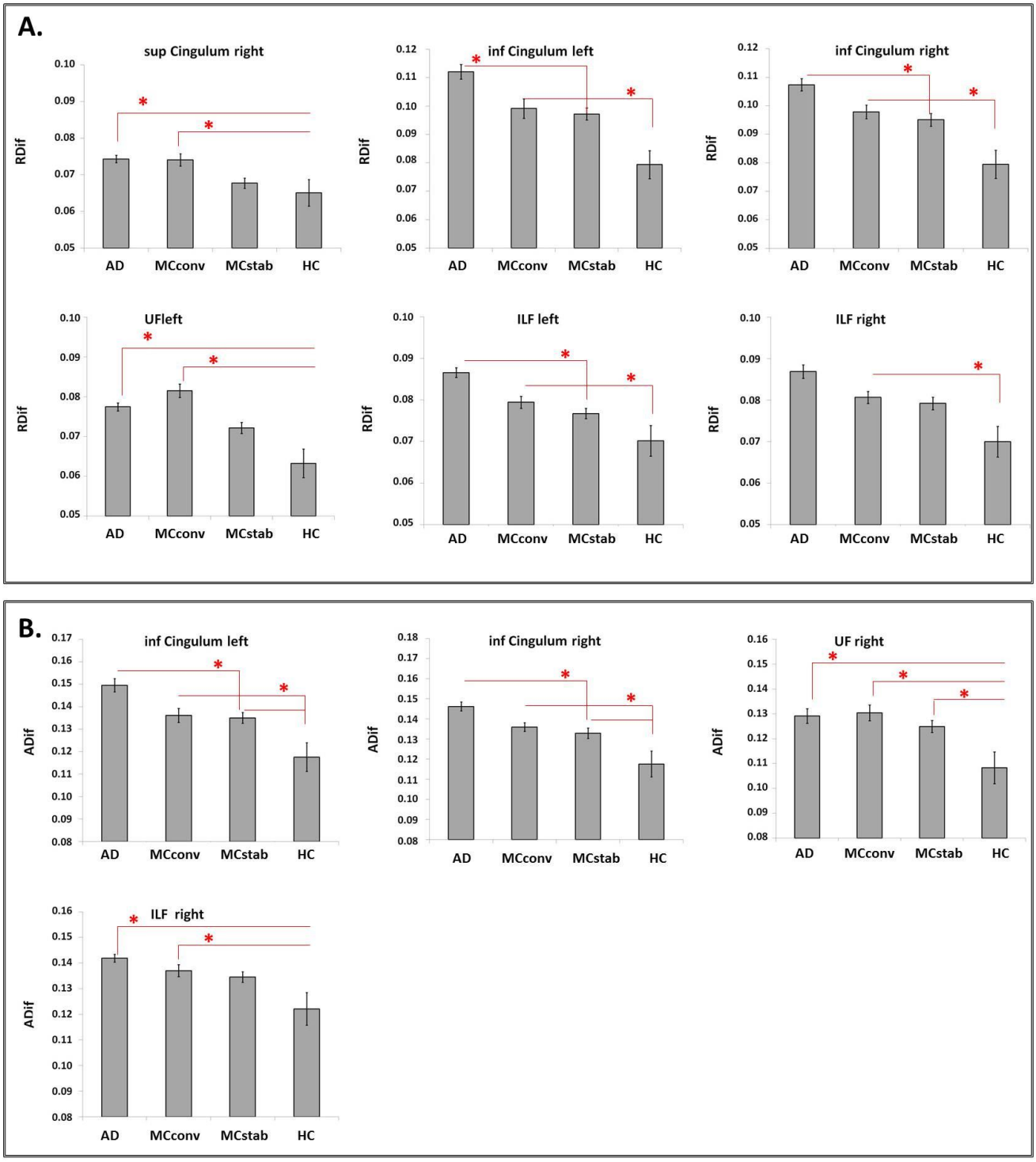


**Figure 2.** Grup-averaged RDif (A) and ADif (B) values in the tracts of interest. Data are reported only for tracts that showed at least one between group significant difference. None of these indices was able to differentiate MCconv from MCstab. Abbreviations: AD= Alzheimer's disease; HC = healthy controls; MCIconv = MCI that converted to AD at follow-up; MCIstab = MCI that remained stable (did not convert to AD) at follow-up; RDif= radial

diffusivity; ADif= axial diffusivity; sup= superior; inf= inferior; UF= uncinated fasciculus; ILF= inferior longitudinal fasciculus.

**Figure 3.**

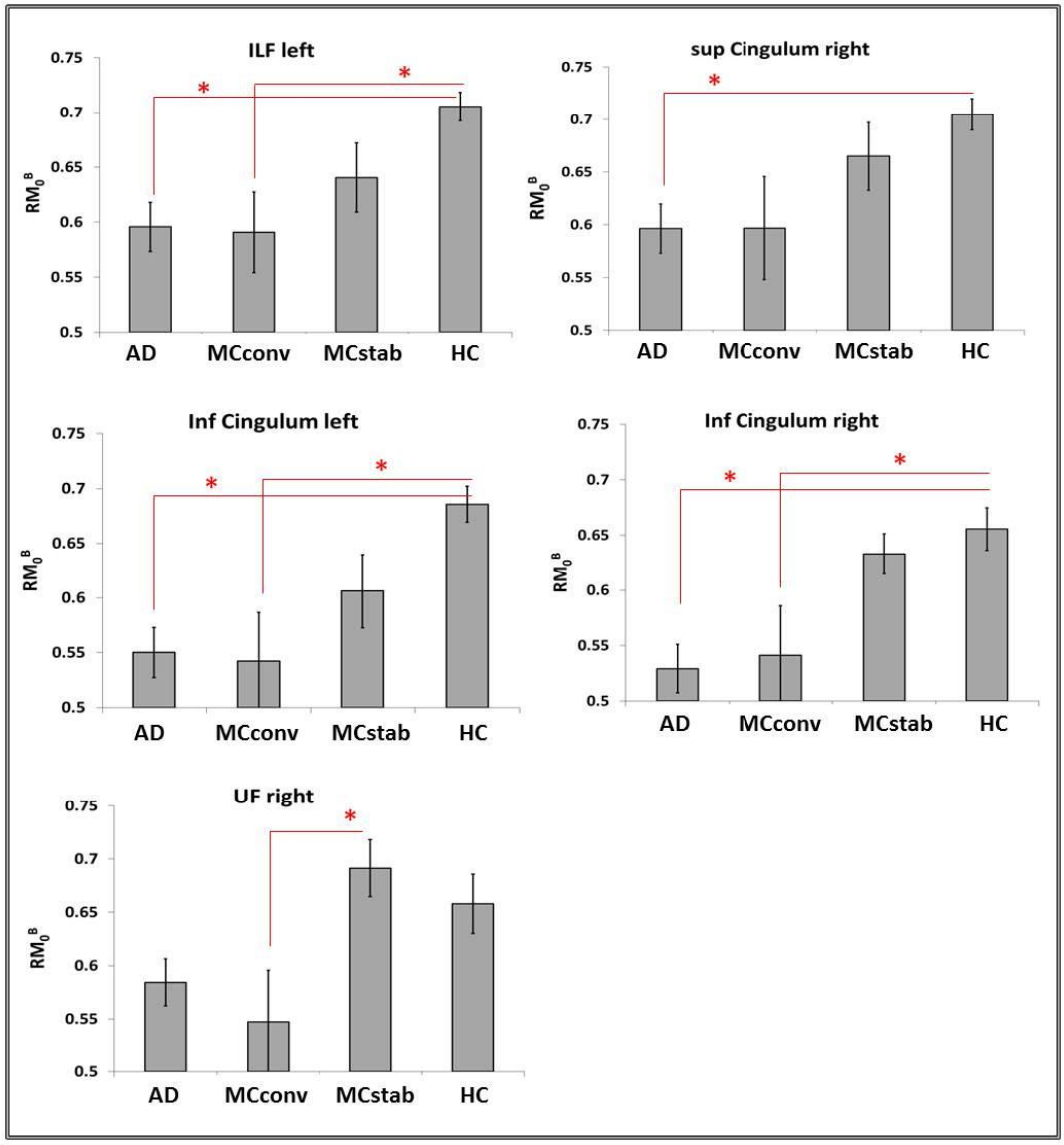


**Figure 3.** Group-averaged Graph $RM_0^B$ values estimated in the tracts of interest. $RM_0^B$ in UF differentiated MCIconverters from MCIstable already at baseline. Abbreviations: AD= Alzheimer's disease; HC = healthy controls; MCIconv = MCI that converted to AD at follow-up; MCIstab = MCI that remained stable (did not convert to AD) at follow-up; $RM_0^B$ = forward exchange rate; sup= superior; inf= inferior; UF= uncinated fasciculus.

**Table 1.**

**Principal demographic and clinical characteristics of the studied subjects**

| | | | MCI | |
|---|---|---|---|---|
| | **AD** | **HC** | **Converters** | **Stable** |
| **Mean (SD) age at scan (years)** | 70.77(7.07) | 61.48 (6.97) * | 61.00 (23.83) * | 65.88 (16.10) |
| **Sex (F/M)** | 29/26 | 12/19 | 12/5 | 7/10 |
| **Mean (SD) years of formal education** | 9.44 (4.19) | 13.86 (3.26) * | 7.23 (5.04) # | 10.75 (4.83) |
| **Mean (SD) MMSE score** | 19.11 (3.80) | 29.39 (1.03) * | 25.42 (2.57) * # | 27.23 (1.94) * |
| **IADL** | 5.03 (1.97) | 0.00 | 6.64 (1.73) | 6.33 (1.63) |
| **Mean (SD) CDR score** | 1.19 (0.67) | 0.00 | 0.50 (0.19) | 0.50 (0.02) |

All vs. AD *; MCI (converters, stable) vs. HC #; MCIconverters vs. MCIstable ^. AD= Alzheimer's disease; HC = healthy controls; MCI = mild cognitive impairment.

**Table 2.**

**Performance scores obtained by HC, AD and MCI patients**

| Domain | Test | AD | HC | MCI | |
|---|---|---|---|---|---|
| | | | | Converters | Stable |
| **Long Term Memory:** | | | | | |
| -Verbal | **15-Words List:** | | | | |
| | Immediate recall (cut-off ≥ 28.5) | 21.33 (9.13) | 46.26 (8.58) | 28.19 (5.84) * # | 32.88 (7.35) * # |
| | Delayed recall (cut-off ≥ 4.6) | 1.79 (1.97) | 9.82 (2.04) | 3.32 (2.60) # ^ | 5.53 (1.88) * # |
| | **Short Story test:** | | | | |
| | Immediate recall (cut-off ≥ 3.1) | 1.91 (2.00) | 6.48 (1.24) | 3.43 (2.80) | 4.91 (1.58) * |
| | Delayed recall (cut-off ≥ 2.9) | 0.95 (1.83) | 6.21 (1.05) | 2.63 (2.40) * # | 4.43 (2.03) * # |
| -Visuo-spatial | **Complex Rey's Figure:** | | | | |
| | Immediate recall (cut-off ≥ 6.4) | 3.73 (4.29) | 15.39 (7.30) | 9.29 (7.48) # | 12.73 (8.07) |
| | Delayed recall (cut-off ≥ 6.3) | 3.48 (4.58) | 14.39 (5.83) | 8.20 (7.00) # | 12.15 (5.57) |
| **Short-term memory:** | | | | | |
| -Verbal | Digit span (cut-off ≥ 3.7) | 4.97 (1.19) | 5.75 (0.98) | 4.63 (1.12) # | 5.19 (0.94) |

| | | | | | |
|---|---|---|---|---|---|
| -Visuo-spatial | Corsi span (cut-off ≥ 3.5) | 3.28 (1.44) | 4.99 (0.82) | 3.97 (0.72) | 4.44 (0.43) * |
| **Executive functions:** | Phonological Word Fluency (cut-off ≥ 17.3) | 21.96 (10.72) | 36.04 (8.28) | 29.88 (6.63) * | 34.78 (10.38) * |
| | Digit span backward | 2.76 (1.60) | 4.75 (0.85) | 3.35 (0.70) # | 3.94 (0.75) * |
| | Corsi span backward | 2.15 (1.84) | 6.69 (8.36) | 3.44 (0.96) | 4.29 (0.69) |
| **Language:** | Naming of objects (cut-off ≥ 22) | 20.92 (10.14) | 29.15 (1.14) | 27.71 (2.08) | 28.82 (1.47) |
| **Reasoning:** | Raven's Coloured Progressive Matrices (cut-off ≥ 18.9) | 21.29 (6.57) | 31.06 (5.53) | 25.28 (4.08) # | 28.99 (4.39) * |
| **Constructional praxis:** | Copy of Drawings (cut-off≥7.1) | 6.42 (3.72) | 11.04 (1.16) | 8.94 (1.45) | 10.19 (1.36) * |
| | Copy of Drawings with landmarks (cut-off≥61.8) | 50.28 (22.92) | 69.20 (0.90) | 65.31 (4.54)* | 67.66 (2.86) * |
| | Copy of Complex Rey's Figure (cut-off ≥ 23.7) | 18.26 (12.66) | 32.67 (2.57) | 25.39 (9.36) | 32.46 (4.53) * |

MCI (conv, stab) vs. AD *****; MCI (converters, stable) vs. HC **#**; MCIconverters vs. MCIstable ^. AD= Alzheimer's disease; HC = healthy controls; MCI = mild cognitive impairment. For each studied group mean (SD) scores obtained in each administered test are reported. For each administered test appropriate adjustments for gender, age and education level were applied according to the Italian normative data. Available cut-off scores of normality (≥95% of the lower tolerance limit of the normal population distribution) are also reported for each test.

**Table 3. Correlation between DTI (FA, MD, RDif, ADif) and qMT (F, $RM_0^B$) indeces.**

| | | | F | $RM_0^B$ | | | | F | $RM_0^B$ |
|---|---|---|---|---|---|---|---|---|---|
| **supCi Left** | **FA** | r | .161 | .131 | **supCi Right** | **FA** | r | .252* | .072 |
| | | *p* | .119 | .206 | | | *p* | .013 | .482 |
| | **MD** | r | -.264** | -.488** | | **MD** | r | -.235* | -.413** |
| | | *p* | .010 | .000 | | | *p* | .021 | .000 |
| | **ADif** | r | -.100 | -.143 | | **ADif** | r | -.125 | -.198 |
| | | *p* | .339 | .172 | | | *p* | .232 | .057 |
| | **RDif** | r | -.173 | -.276** | | **RDif** | r | -.214* | -.259* |
| | | *p* | .098 | .008 | | | *p* | .040 | .012 |
| **infCi Left** | **FA** | r | -.031 | .187 | **infCi Right** | **FA** | rr | .040 | .012 |
| | | *p* | .761 | .066 | | | *p* | .697 | .910 |
| | **MD** | r | -.188 | -.600** | | **MD** | r | -.053 | -.389** |
| | | *p* | .065 | .000 | | | *p* | .613 | .000 |
| | **ADif** | r | -.085 | -.480** | | **ADif** | r | .004 | -.300** |
| | | *p* | .414 | .000 | | | *p* | .968 | .004 |
| | **RDif** | r | -.114 | -.517** | | **RDif** | r | -.038 | -.275** |
| | | *p* | .274 | .000 | | | *p* | .720 | .008 |
| **UF Left** | **FA** | r | .373** | .172 | **UF Right** | **FA** | r | .191 | .229* |
| | | *p* | .000 | .097 | | | *p* | .066 | .027 |
| | **MD** | r | -.247* | -.067 | | **MD** | r | -.231* | -.465** |
| | | *p* | .016 | .520 | | | *p* | .026 | .000 |
| | **ADif** | r | -.127 | -.228* | | **ADif** | r | -.025 | -.235* |
| | | *p* | .224 | .028 | | | *p* | .817 | .025 |
| | **RDif** | r | -.283** | -.319** | | **RDif** | r | -.119 | -.467** |
| | | *p* | .006 | .002 | | | *p* | .261 | .000 |
| **ILF Left** | **FA** | r | .130 | .274** | **ILF Right** | **FA** | r | .204* | .271** |
| | | p | .208 | .007 | | | p | .047 | .008 |
| | **MD** | r | -.023 | -.349** | | **MD** | r | -.014 | -.165 |
| | | p | .821 | .000 | | | p | .889 | .107 |
| | **ADif** | r | .025 | -.162 | | **ADif** | r | .052 | -.051 |
| | | p | .813 | .116 | | | p | .614 | .626 |
| | **RDif** | r | -.023 | -.294** | | **RDif** | r | -.020 | -.149 |
| | | p | .823 | .004 | | | p | .844 | .150 |

Fractional anisotropy=FA, Mean diffusivity=MD, Radial diffusivity=RDif, Axial diffusivity=ADif, forward exchange rate=$RM_0^B$, relative size of the macromolecular pool=F; supCi= superior cingulum; infCi= inferior cinguilum; UF= uncinated fasciculus; ILF= inferior longitudinal fasciculus. Significant p-values are printed in red

**Acknowledgements**

This project has been supported by grants of the Italian Ministry of Health and of the Italian Ministry of University and Research.

**Disclosure Statement**

None of the authors has any actual or potential conflict of interest including any financial, personal or other relationships with other people or organizations within three years of beginning the work submitted that could inappropriately influence (bias) their work. The study was approved by the local ethics committee before initiation. All subjects gave written informed consent before taking part in the study.